SEGMENTATION OF 3D HEAD MR IMAGES USING MORPHOLOGICAL RECONSTRUCTION UNDER CONSTRAINTS AND AUTOMATIC SELECTION OF MARKERS

*Petr Dokládal, Raquel Urtasun, Isabelle Bloch**

Ecole Nationale Supérieure des Télécommunications
CNRS URA 820 - Dept TSI
46 rue Barrault, 75013 Paris, France
Isabelle.Bloch@enst.fr

Line Garnero

LENA - CNRS UPR 640
Hôpital La Salpétrière
75651 Paris Cedex 13, France

ABSTRACT

We propose in this paper a morphological approach to segment several structures of 3D head magnetic resonance images dedicated to the construction of individual models of the head for applications where topology is one of the main constraints. The originality of the approach lies in the satisfaction of such constraints and in a effort towards robustness.

1. INTRODUCTION

A large body of literature has been devoted to brain image segmentation (see e.g. the synthesis in [1]). We will deal here with magnetic resonance images (MRI). A lot of classification methods have been developed to separate the main tissues. For instance, both fuzzy clustering and neural networks have been widely used, as well as probabilistic approaches. Other methods make use of models. These models can be implicit like Physics-based deformable models or explicit as in atlas deformation techniques. Implicit models are often used when one specific structure of interest has to be detected, while atlas-based approaches can segment all structures but have to deal with difficult problems due to the anatomical variability. Here we are interested in methods without model that exploit not only the content of the image but also constraints on the desired result, as topological constraints. Classification methods can hardly incorporate such constraints, while morphological methods are more adapted to this aim. Most work using mathematical morphology in this domain concentrate on segmentation of the brain and on separation between grey and white matter e.g. [2, 3, 4]. Little attention was paid to the other structures until now. For instance very few methods exist for skull and skin, and they usually rely on different constraints from the ones we have here (see e.g. [5]).

Here, based on a preliminary segmentation of the brain, we propose a morphological method to segment the brain stem and the cerebellum, cerebrospinal fluid (CSF), grey and white matter, skull and scalp. The aim of this segmentation is to build from any standard MRI an individual 3D model of head structures, that can serve for numerical solving of electromagnetic wave propagation equations, as needed in electrophysiology as well as when studying the influence of mobile phones on head tissues. In contrary to other applications where a millimetric precision may be needed, for such applications the precision of the segmentation is not the key point. What is the most important for the foreseen applications is to have a good and robust representation of the shapes and a very strong constraint is the preservation of topology. Robustness is achieved in the proposed morphological approach by an intensive use of reconstruction and conditional operations as well as by reducing the number of parameters, while the topology is preserved using homotopic transformations. An important aspect of the proposed method is the automatic selection of markers that avoids user interaction and also increases robustness. The method has been successfully applied to 13 3D MR images from different acquisition devices.

The paper is organized as follows. In Section 2 we recall some basic notions related to homotopic morphological operations. We propose a way to select automatically a given number of markers, and homotopic deformations that combine topological and other criteria (on distance or on grey levels for instance). In Section 3, we present successively methods for segmenting the structures of interest. Then experimental results are given in Section 4, along with some comments on parameter estimation and robustness.

2. MORPHOLOGICAL OPERATORS UNDER ROBUSTNESS AND TOPOLOGICAL CONSTRAINTS

We use the following notations. Let $f : \mathbb{Z}^3 \to \mathbb{N}$ denote a discrete image. Let $\delta_\Gamma(f)$ denote a dilation of f by a structuring element Γ, $\Gamma \subset \mathbb{Z}^3$: $\delta_\Gamma(f)(x) = \bigvee_{x_i \in \Gamma(x)} f(x_i)$, where $\Gamma(x)$ denotes the translation of Γ at x. We denote by $\varepsilon_\Gamma(f)$ the erosion of f by Γ, by $\gamma_\Gamma(f)$ the opening and by $\varphi_\Gamma(f)$ the closing. For any subset X of $\mathbb{Z}^3$, $\overline{X}$ denotes the complement of X. The function dist : $\mathbb{Z}^3 \times \mathbb{Z}^3 \to \mathbb{N}$, denotes an approximation of the Euclidean distance in $\mathbb{Z}^3$. We use the same notation for the distance of a point to a set. The function dist_g^X denotes the geodesic distance, calculated within the set X.

2.1. Morphological reconstruction

Reconstruction is one classical way in mathematical morphology to achieve robustness by conditioning transformations to a reference set or image, and therefore controlling the spatial extensions of the transformations [6, 7]. Geodesic transformations are defined by using balls of the geodesic distance as structuring elements. In the discrete case, a geodesic dilation of a set Y conditionally to a set X by a ball of radius 1 is simply computed as [7]:

* Thanks to RNRT Project COMOBIO for partial funding of this work. See http://www.tsi.enst.fr/comobio/

$\delta_g^X(Y) = \delta(Y) \cap X$, where δ_g^X uses the geodesic ball of radius 1 as structuring element and δ the Euclidean ball of radius 1. The reconstruction of Y in X is then defined by iterating this conditional dilation until convergence: $(\delta(Y) \cap X)^\infty$ (note that convergence is achieved in a finite number of steps for X finite). These definitions extend to functions and the reconstruction of f' under f is defined as $(\delta(f') \wedge f)^\infty$. The other geodesic morphological operations are defined in a similar way.

2.2. h-minima, graph representation and automatic selection of markers

The h-minima operator (see e.g. [7]) can be used to find in a function the set of all markers identifying attraction basins, the depth of which exceeds h. In some applications, however, one may need to find a given number of markers without knowing the corresponding value of h. We propose here a way to determine automatically a given number of markers, that may possibly correspond to different unknown depths h, by considering a graph representation of a function and its local minima.

Let f denote a function $f : \mathbb{Z}^3 \to \mathbb{N}$ and $h \in \mathbb{N}$. Let $M \subset \mathbb{Z}^3$ such that $M = \{x | f(x) < h\}$. Let M_i denote a connected component of M. These components for all possible values of h are organized in a weighted tree (see Fig. 1). Every vertex represents one component (given by dashed line); the weights of the vertices correspond to the value of h giving birth to the component. The edges represent the inclusion relation. This tree can be simplified

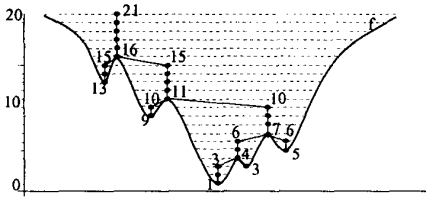

Fig. 1. 1-D example of function f and the component tree (not all weights are given).

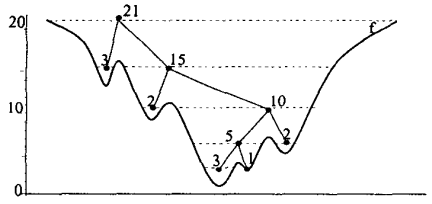

Fig. 2. Simplified component tree.

by deleting every vertex that is a unique child of its parent, i.e. not modifying the topology. The weights are recalculated as follows: every vertex gets the difference of its previous value and their most distant descendant plus one (see Fig. 2). The surviving vertices represent the largest components M_i before the topology of the cuts changes as h increases. The new values correspond to the depths of the associated basin.

The search of the n deepest basins reduces to the search of the n vertices having the highest weights that are not bound (even transitively) by the inclusion relation.

2.3. Homotopic transformations under constraints

Homotopic transformations can be performed in discrete spaces thanks to the use of simple points (e.g. [8, 9]), i.e. that can be deleted from a set X (or added to X) without modifying its topology. Any transformation which acts exclusively on simple points is therefore homotopic. Selection of simple points belongs to the class of hit-or-miss transformations, while deleting simple points from X (respectively adding to X) belongs to the class of morphological thinnings (respectively thickenings). In order to guarantee a topologically consistent result, we extensively use homotopic deformations throughout the segmentation process. These deformations are implemented by two dual operators λ-thinning and λ-thickening [10]. These operators perform a homotopic thinning (resp. thickening) of some binary object according to some criterion λ. This criterion can be of any nature, not necessarily a topological one. Therefore λ-thinning and λ-thickening allow to perform transformations combining topological constraints with any other constraint. Moreover, it is known that the result of thinning or thickening depends on the order points are tested. Here the order is given by the satisfaction of the constraint λ. For instance, λ can be a criterion on grey levels, as $f(x) < C$, and points are ordered by their grey level. Then if X denotes some initial binary object, the λ-thinning iteratively deletes from X all simple points such that $f(x) < C$. The darkest simple points are deleted first. The λ-thickening operator is defined from λ-thinning by duality with respect to complementation, and iteratively adds points to X according to criterion λ.

3. SEGMENTATION METHOD

We start from the mask of the encephalon X_{ENCEPH} which has been obtained by 3D morphological operators (see [11] for details on the method). X_{ENCEPH} is a smooth envelop of the brain including CSF.

3.1. Brain stem and cerebellum

The segmentation of the cerebellum and the brainstem is generally not addressed in the literature. We base it on bottleneck constriction. These objects are separated from each other and from the encephalon at the narrowest junction situated in the mesencephalon and in the cerebral peduncles.

Firstly, we obtain the starting object: $X_1' = \{x \,|\, x \in X_{ENCEPH} \text{ and } f(x) > s_1\}$, where $s_1 = \mu_{CORTEX}$ is the mean value of the grey matter. From now on, we only consider the lower part of X_1' limited on top by the higher extremity of the tegmentum. This can be easily found manually. Let X_1 denote the resulting object.

The separation proceeds in two steps. Firstly, we identify the lateral lobes which have to be deleted. The narrow junctions of some object X are identified as topographic saddles of the distance function to $\overline{X_1}$: $g_1 = \text{dist}(x, \overline{X_1})$. We search three markers $M = \{M_1, M_2, M_3\}$ corresponding to the three most significant basins of $-g_1$ using the method described in Section 2. The objects are obtained by homotopic reconstruction of the 3 markers in g_1: $X_2 = \lambda\text{-thickening}(M), \lambda : g_1(x) > 0$ (see Section 2). The largest connected component of X_2 is the union of the cerebellum and the brainstem: X_{BS+CB}. Due to the structure of the cerebellum, we perform a binary morphological closing in order to obtain a smooth-surfaced object $\varphi_\Gamma(X_{BS+CB})$. The structuring element Γ is a ball of radius $R = 1$ mm.

The second step separates the brainstem and the cerebellum. The separation is based on the localization of the narrow junctions identified as saddles in the distance function $g_2 = \text{dist}(x, \overline{\varphi_\Gamma(X_{BS+CB})})$. We search three markers $M = \{M_1, M_2, M_3\}$ marking the most significant basins of $-g_2$. By reconstruction of M we obtain $X_3 = \lambda\text{-thickening}(M)$, λ: $g_2(x) > 0$. The brainstem X_{BS} is the smallest connected component of $X_3 \cap X_{BS+CB}$. The cerebellum X_{CB} is obtained as the union of the two largest connected components of $X_3 \cap X_{BS+CB}$. We obtain the hemispheres by $X_{HEMISPH} = X_{ENCEPH} \setminus X_{BS} \setminus X_{CB}$.

The proposed method relies on the fact that we have a prior knowledge of the number of objects in interest, and from the automatic selection of a corresponding number of markers, chosen as the most significant ones.

3.2. Cerebrospinal fluid

This method extracts the object X_{CSF} contained both in the ventricles and in the sulci. We impose to X_{CSF} the topology of a hollow sphere. It corresponds to the reality but not necessarily to the input image because of limited resolution. This is a specificity of the proposed approach, to include constraints related to reality or to further applications, even if the data do not satisfy them.

We start with an initial thresholding: $X_4 = \{x \mid x \in X_{ENCEPH} \text{ and } f(x) < s_2\}$ where $s_2 = \mu_{CSF} + 2\sigma_{CSF}$, and μ_{CSF} and σ_{CSF} are the mean and the standard deviation of CSF. Then we filter out noisy points by opening: $X_5 = X_4 \setminus \gamma_\Gamma(X_4)$ where Γ is a ball of radius $R = 1$ mm. We define a new image g as:

$$g(x) = \begin{cases} f(x) & \text{if } x \in X_4 \text{ and } x \in X_5 \\ s_2 & \text{if } x \in X_4 \text{ and } x \notin X_5 \\ 0 & \text{else} \end{cases}$$

We extract X_{CSF} by reconstruction of $\overline{X_{CSF}}$. Let $X_6 = \lambda\text{-thickening}(M)$ where $\lambda : g(x) \geq s_2$, where the marker M is an arbitrary point of the encephalon X_{ENCEPH} such that $f(x) > s_2$ (i.e. in $\overline{X_{CSF}}$). CSF is then obtained by complementation: $X_{CSF} = \delta_\Gamma(X_{ENCEPH}) \setminus X_6$, where Γ is a ball of radius $R = 1$ mm. The dilation guarantees that X_{CSF} contains all CSF.

From now on we consider X_{ENCEPH} as $X_{ENCEPH} \setminus X_{CSF}$.

3.3. Grey and white matter

The segmentation of grey and white matter are initialized from a classical k-means classification algorithm. Then, starting from the largest component of white matter, the interface between white and grey matter is obtained by λ-thickening in the complement of grey matter and with a constraint λ giving priority to the simple points which are at the smallest geodesic distance from the initialization. The interface between grey matter and CSF is obtained in a similar way, by λ-thickening in the complement of CSF, with the same priority depending on geodesic distances.

3.4. Skull

The extraction of skull is subject to two constraints: 1) the object X_{SKULL} is homotopic to a hollow sphere (note that this is a constraint imposed by the applications and not corresponding exactly to the reality; it is completely different from the one of [5] where no precise topology is required), 2) regions situated far from the cortical surface are eliminated. The segmentation proceeds in two steps according to these requirements: presegmentation and hole (tunnel) closing.

1) Masking of the encephalon and the air. We first define $X_7 = f \cap (X_{HEAD} \setminus X_{ENCEPH})$. Then by thresholding we get $X_8 = \{x \mid x \in X_7 \text{ and } f(x) < s_3\}$, where $s_3 = \mu_{CORTEX} - \sigma_{CORTEX}$. A mask close to the cortex is defined as $X_{MASK} = \delta_\Gamma(X_{HEMISPH} \cup X_{CB})$, where Γ is a ball of $R = 25$ mm; $X'_{SKULL} = X_8 \cap X_{MASK}$. The mask includes the skullcap, the front and the cranium base. The sinus and jaw are suppressed.

2) Hole closing. We use a modified version of the hole closing algorithm of [12] based on homotopic deformations controlled by a distance function from the object. The starting object X_9 has the correct topology and is homotopically deformed towards the desired result. The deformation keeps the holes closed. Since the deformation is controlled by the distance, the holes are closed with a minimal surface. Then $X_9 = X_{MASK} \setminus (X_{HEMISPH} \cup X_{CB})$ contains the skull and has one cavity, which is the desired topology. From the distance function $d(x) = \text{dist}(x, X'_{SKULL})$, the skull is obtained by homotopic thinning: $X_{SKULL} = \lambda\text{-thinning}(X_9)$, $\lambda : d(x) > 0$.

3.5. Skin

The first step consists in extracting the head mask X_{HEAD}. This object is simply connected with no holes nor cavities. After an initial thresholding and selection of the greatest connected component leading to $X_{10} = \text{MaxCC}(\{x \mid f(x) > s_3\})$ where $s_3 = \mu_{CSF} - \sigma_{CSF}$, we perform a smoothing by a morphological closing: $X_{11} = \varphi_\Gamma(X_{10})$, Γ : ball of $R = 5$mm. Filling of cavities leads to $X_{12} = \text{Fill}(X_{11})$. The object X_{12} is too smooth and does not follow correctly the head contours. Therefore we propose to add a peeling step eliminating dark regions introduced by the closing. The closing, however, cannot be omitted since its purpose is to close the orifices (ears...) which would have otherwise connected the exterior of the head with the bone, the air and the bone having the same luminosity. The peeling is only limited to dark points (the air) and up to some maximum distance from the surface of X_{HEAD}. A geodesic transform can be used $g(x) = \text{dist}_g^{\overline{X_{10}}}(\overline{X_{12}})$, and peeling is achieved by $\lambda\text{-thinning}(X_{12}) = X_{HEAD}$ where $\lambda : g(x) < R$, where R is the radius used in the closing (5 mm). X_{HEAD} has therefore the correct topology and its surface follows the contour of the head.

The skin X_{SKIN} is obtained in the next step by thickening of the border of the head mask $\text{bd}(X_{HEAD})$. The thickening is bounded by a maximum distance from the contour and is limited to bright points only, likely to belong to the skin. This restriction is achieved by a geodesic transform $g(x) = \text{dist}_g^{\overline{X_{10}}}(\overline{X_{HEAD}})$.

Homotopic thickening of the contour of the head: $X_{SKIN} = \lambda\text{-thickening}(\text{bd}(X_{HEAD}))$, where $\lambda : g(x) < C$, where $C =$ 6mm (maximum allowed thickness of the skin and epidermis). The thickening extends homotopically the head contour inwards. X_{SKIN} has the topology of a hollow sphere and entirely covers the head. The orifices are covered by an one-point-thick surface.

4. EXPERIMENT RESULTS

4.1. Parameter estimation and robustness

The segmentation algorithm uses several parameters. Grey level parameters are estimated automatically with the k-means algorithm, with $k = 5$ (for air and bone, cerebrospinal fluid, grey

matter, white matter, fat). The mean values μ_i and standard deviations σ_i are calculated for each of the five classes found by the k-means. Sometimes (about 30 percent of all cases) the k-means fail to identify the cerebrospinal fluid (due to the partial volume effect and negligible volume occupied by this structure compared to other objects). A manual intervention is therefore needed to verify the result of the k-means. No other user-interaction is needed, except for designing the horizontal slice used to segment the cerebellum and the brain stem. We have shown experimentally that the results are robust to variations of the position of this slice (any of 5 successive slices can be chosen without changing the results). The sizes of the structuring elements are derived from anatomical knowledge and the same values could be successfully used on all examples. Markers are selected automatically, and geodesic transformations and reconstruction contribute to robustness of the method.

4.2. Results

We have tested the segmentation of thirteen MR images of the head (Fig. 3 gives an example of the input MRI). Despite the diversity of the input images, the method exhibits a good robustness. The result is a partition of the space and its 3D topology is guaranteed. These results have been positively evaluated by medical doctors and electrophysiologists and are now used as individual models for solving equations of electromagnetic wave propagation in head tissues.

Fig. 3. 2D orthogonal slices from an example input image.

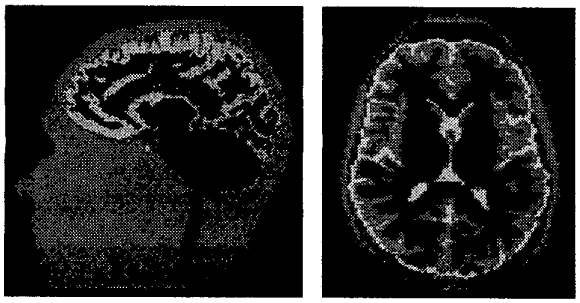

Fig. 4. Result of segmentation of the image given in Fig. 3.

5. CONCLUSION

Although different works addressed brain segmentation, the foreseen applications called for other methods focusing on the topology of the result. The originality of the proposed approach is to provide an automatic and robust method devoted to specific applications. The constraints are derived from the application and are guaranteed even if they are not completely true in reality or in the data. The reduced number of parameters, the automatic selection of markers and the use of morphological reconstruction contribute to the increase in robustness.

6. REFERENCES

[1] L.P. Clarke, R.P. Velthuizen, M.A. Camacho, J.J. Heine, M. Vaidyanathan, L.O. Hall, R.W. Thatcher, and M.L. Silbiger, "MRI Segmentation: Methods and Applications," *Journal of Magnetic Resonance Imaging*, vol. 13, no. 3, pp. 343–368, 1995.

[2] S. Sandor and R. Leahy, "Surface-Based Labeling of Cortical Anatomy Using a Deformable Model," *IEEE Transactions on Medical Imaging*, vol. 16, no. 1, pp. 41–54, Feb. 1997.

[3] J. F. Mangin, V. Frouin, I. Bloch, J. Regis, and J. Lopez-Krahe, "From 3D Magnetic Resonance Images to Structural Representations of the Cortex Topography using Topology Preserving Deformations," *Journal of Mathematical Imaging and Vision*, vol. 5, pp. 297–318, 1995.

[4] C. Tsai, B.Manjunath, and R. Jagadeesan, "Automated Segmentation of Brain MR Images," *Pattern Recognition*, vol. 28, pp. 1825–1837, 1995.

[5] H. Rifai, I. Bloch, S. Hutchinson, J. Wiart, and L. Garnero, "Segmentation of the Skull in MRI Volumes Using Deformable Model and Taking the Partial Volume Effect into Account," *Medical Image Analysis*, vol. 4, no. 3, pp. 219–233, 2000.

[6] J. Serra, *Image Analysis and Mathematical Morphology*, Academic Press, London, 1982.

[7] M. Schmitt and J. Mattioli, *Morphologie mathématique*, Masson, Paris, 1994.

[8] G. Bertrand, "On P-Simple Points," *C. R. Acad. Sci. Paris.*, vol. Serie 1, pp. 1077–1084, 1995.

[9] A. Rosenfeld, T.Y. Kong, and A. Nakamura, "Topology-Preserving Deformations of Two-Valued Digital Pictures," *Graphical Models and Image Processing*, vol. 60, no. 1, pp. 24–34, Jan. 1998.

[10] P. Dokládal, *Segmentation des images en niveaux de gris : une approche topologique*, Ph.D. thesis, Université Marne la Vallée, janvier 2000.

[11] T. Géraud, *Segmentation des structures internes du cerveau en imagerie par résonance magnétique tridimensionnelle*, Ph.D. thesis, École Nationale Supérieure des Télécommunications, ENST 98E012, jun 1998.

[12] Z. Aktouf, G. Bertrand, and L. Perroton, "A 3D Hole Closing Algorithm," in *6th workshop on Discrete Geometry for Computer Imagery*, November 1996.